IFSCC 2025 full paper (IFSCC2025-306)

A supramolecular salicylic acid with low irritation and enhanced anti-acne ability

Zhenyuan Wang [1], Zhixuan Han [1], Mi Wang [2,*], Qingsheng Tao [3], Hao Wang [2], Mei Zhang [3], Xueli Liu [3], Jichuan Zhang [2] and Jiaheng Zhang [1,2,*]

1 Shenzhen Shinehigh Innovation Technology, Co., Ltd., Shenzhen, China
2 Sauvage Laboratory for Smart Materials, School of Material Sciences and Engineering, Harbin Institute of Technology (Shenzhen), Shenzhen, China
3 Advanced Research, L'Oreal Research & Innovation China, Shanghai, China

---

1. Introduction

Salicylic acid (SA) is a lipophilic compound widely used in dermatology. It offers multifaceted therapeutic benefits such as sebum modulation, exfoliation, follicular clearance, and anti-inflammatory/antibacterial effects, establishing it as a cornerstone in acne treatment [1–4]. However, its clinical utility is limited by poor solubility, formulation instability, and side effects like irritation.

Crystallization technology enables precise modulation of drug properties through cocrystal engineering, enhancing solubility, stability, and tolerability [5,6]. In a previous study, we successfully prepared supramolecular crystals of an ion salt by creating a complex of SA and matrine [7]. It demonstrated significantly enhanced solubility, transdermal permeability, and safety in comparison to pure SA. However, limited plant sources and the high price of matrine resources call for further exploration or alternative solutions

In parallel, betaine, a cost-effective zwitterionic alkaloid from sugar beets, exhibits exceptional biocompatibility, hygroscopicity (stabilizing 12 water molecules) [8], osmotic regulation [9], and UV-protective antioxidant activity [10]. These attributes position betaine as an ideal candidate for improving the tolerability and efficacy of topical therapeutics.

Acne is a skin condition with a relatively high prevalence, reaching 80% – 90% during adolescence, while that during adulthood is relatively low, usually between 20%–40% [11]. The integration of SA with betaine via cocrystallization presents a promising avenue to synergize their complementary properties for acne management. Cocrystals are capable of mitigating the irritancy of SA by decreasing its local concentration, while maintaining or enhancing its bioactivity. Betaine, with its economic viability and proven safety, offers a sustainable solution. By forming hydrogen-bonded networks with SA, betaine may not only enhance the physicochemical properties of SA but also provide intrinsic moisturizing and anti-inflammatory benefits, thereby improving the therapeutic efficacy for acne-prone skin.

In this study, we synthesized a novel betaine-salicylic acid cocrystal (BetSA) systematically. BetSA was characterized via XRD, NMR, FTIR, and single-crystal analysis, alongside thermal profiling (TGA/DSC). Computational simulations and clinical trials evaluated its bioactivity, demonstrating reduced transepidermal water loss, porphyrins, erythema, and acne lesions.

2. Materials and Methods

2.1. Materials

Betaine (≥98%) and salicylic acid (SA, ≥99.5%) were purchased from Aladdin (China). Human keratinocytes (ES190826) and culture medium (KC2500) were sourced from Guangdong Biocell Biotechnology. MTT reagent, ROS/SOD assay kits, and ELISA kits (IL-1α, IL-8) were obtained from Sigma-Aldrich, Beyotime, and Abcam, respectively.

2.2. Preparation of BetSA

Betaine (4 mM) was added to 60 mL of ethanol containing 4 mM SA under stirring. The mixture was stirred at 60°C under N_2 for 24 h. Crystals were collected via rotary evaporation, washed with cold ethanol, and vacuum-dried at 40°C. Single crystals were obtained by slow ethanol recrystallization.

2.3. Characterization

XRD patterns were recorded on a Rigaku D/max 2500PC diffractometer. SEM images were captured using a Hitachi SU8010 microscope. ^{1}H NMR spectra (400 MHz, Bruker) and FTIR spectra (Thermo Nicolet 380) were acquired in deuterated methanol. Thermal properties (T_m, T_d) were analyzed via TGA (PerkinElmer) and DSC (Mettler Toledo). Single-crystal structures were resolved using an Agilent SuperNova diffractometer.

2.4. Cell Experiments

Cytotoxicity of betaine, SA, and BetSA on human keratinocytes was assessed via MTT assay. Neutral red uptake (NRU) tests followed OECD TG 432 using NIH/3T3 fibroblasts. UVB-induced inflammation and oxidative stress models were established. ROS levels were quantified via flow cytometry (Beckman Coulter FC500), while SOD activity, IL-1α, and IL-8 levels were analyzed using commercial kits.

2.5. Computer Simulations

DFT calculations (ORCA 5.0.4) optimized betaine, SA, and BetSA structures at the B97-3c level, with single-point energies evaluated using M062X/6-311++G(d,p) and SMD solvation. ESP, IGMH, AIM, and frontier orbital analyses were performed using Multiwfn/VMD [12]. Molecular docking (AutoDock 4.2.6) and MD simulations (GROMACS 5.0.2) analyzed SA/BetSA interactions with the TIR domain (PDB: IFYV). After 10 ns equilibration, ligand-TIR interactions were evaluated from the final 10 ns trajectory [13].

2.6. Clinical Trials

The test formula is a base formula containing 3 wt% BetSA or an equivalent mass of water (Blank group). Approved trials (MC-GXRT202200044/045) involved 30 acne-prone participants per group (BetSA: 16M/14F, 18–30 years; SA: 13M/17F, 20–35 years). Participants applied samples nightly for 28 days. TEWL, porphyrins, erythema, and acne were measured weekly using a VISIA-CR® scanner after 0.5 h acclimation.

2.7. Statistical Analysis

Data (mean ± SD) were analyzed via GraphPad Prism 9.5. Cell experiments (triplicate) used one-way ANOVA; clinical trials employed paired/unpaired t-tests. Significance was set at $P < 0.05$.

3. Results

3.1. Preparation and characterization of BetSA

The BetSA cocrystal was synthesized via a 1:1 molar ratio of betaine and SA. XRD analysis confirmed a unique crystalline phase distinct from precursors (Fig. 1a), while ^{1}H NMR verified high purity (Fig. 1b). Fourier-transform infrared (FTIR) spectroscopy was employed to analyze the molecular structures. In the FTIR spectrum of SA, a broad absorption band ranging from 2530–3240 cm^{-1} is attributed to O-H stretching vibrations. Additionally, the C=O stretching vibration at 1660 cm^{-1} corresponds to carboxylic acid dimerization (Fig. 1c). In

contrast, betaine shows a broad absorption peak near 3300 cm^{-1}, which is ascribed to moisture adsorption, and a distinct CH_3 stretching peak at 3020 cm^{-1}. Notably, its C=O stretching vibration at 1630 cm^{-1} exhibits a red shift, likely due to intermolecular electrostatic interactions. In BetSA, the O–H stretching band of SA undergoes a blue shift, while the C=O stretching of betaine displays a red shift (Fig. 1c). Thermal analysis reveals that BetSA exhibits a lower melting temperature (T_m = 112°C) and a higher decomposition temperature (T_d = 220°C) compared to its precursors (Fig. 1d).

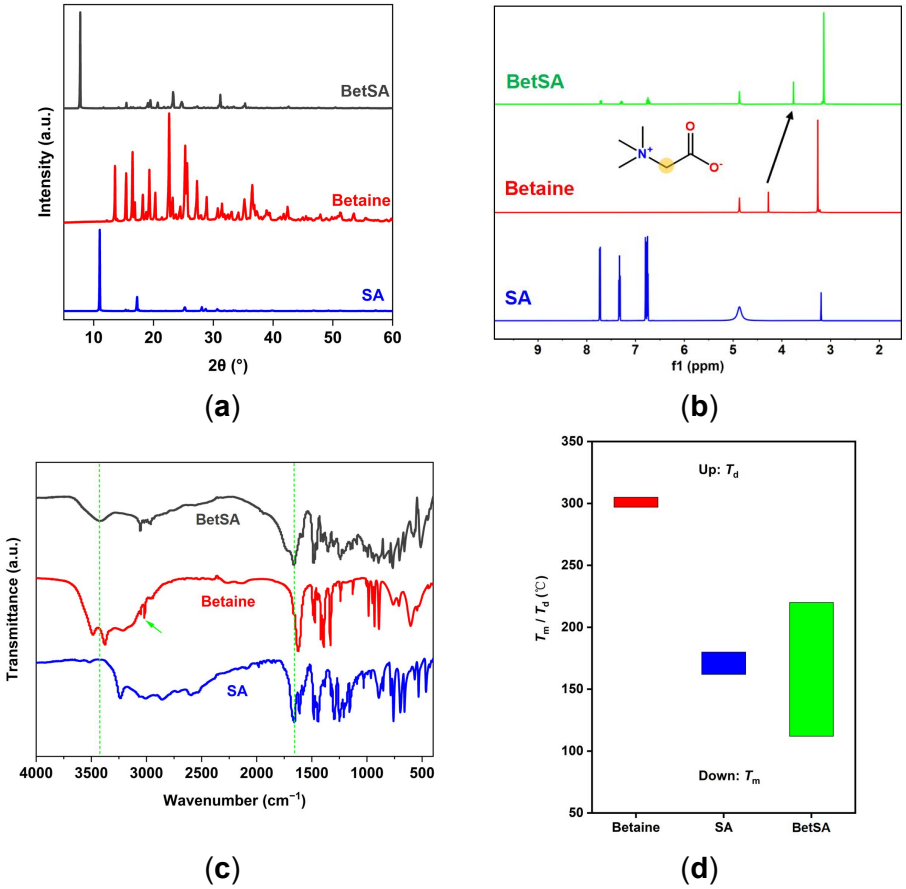

Figure 1. (a) X-ray diffraction (XRD) patterns; (b) ^1H nuclear magnetic resonance spectroscopy (NMR); (c) Fourier-transform infrared (FTIR) spectra; (d) thermal properties of BetSA and its precursor compounds.

Single-crystal X-ray diffraction elucidated the molecular arrangement of BetSA. The BetSA cocrystal belongs to the orthorhombic space group Pbca, with lattice parameters a = 10.211 Å, b = 10.775 Å, and c = 22.531 Å, containing eight BetSA molecules per unit cell (Fig. 2a). Hydrogen bonding between the carboxyl groups of SA and betaine governed the supramolecular architecture. Along the b-axis, BetSA adopted a layered "sandwich" structure, with parallel SA molecules (spaced 5.28 Å apart) interleaved with betaine molecules (Fig. 2b).

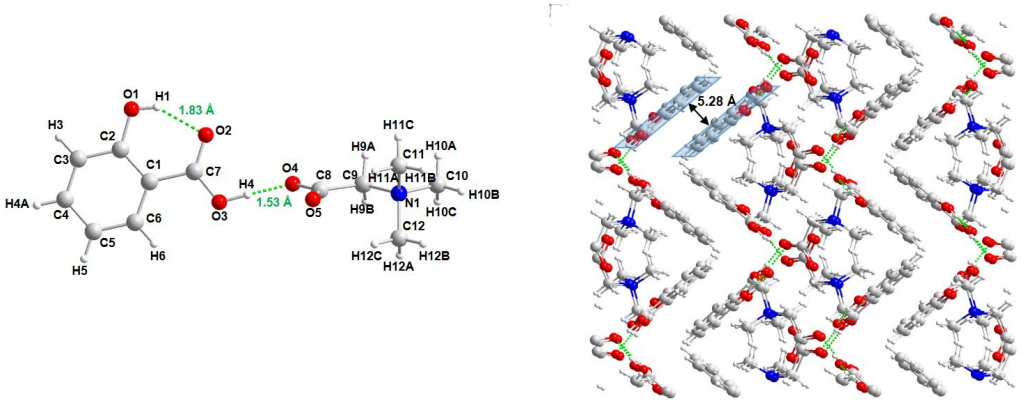

(**a**) (**b**)

Figure 2. (a) Molecular structure of BetSA; (b) Molecular arrangement of BetSA along b-axes, with hydrogen bonds represented by the dotted green lines.

3.2. Bioactivities of BetSA

Safety and efficacy of BetSA were evaluated using cytotoxicity and neutral red uptake (NRU) assays in human keratinocytes. The safe concentration of SA was determined to be 0.004 mg/mL, whereas betaine exhibited a safe concentration of 5 mg/mL. The safe concentration of BetSA was identified as 0.125 mg/mL. NRU tests further confirmed the reduced irritancy of BetSA, with an IC_{50} value more than threefold higher than that of SA, and no phototoxicity was observed (Fig. 3a-b).

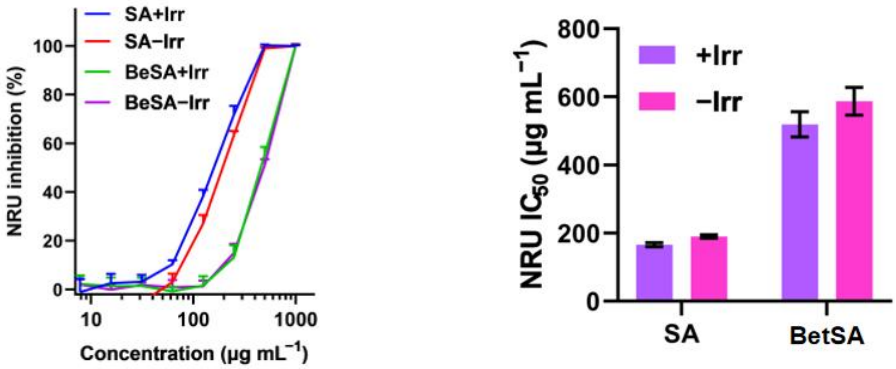

(**a**) (**b**)

Figure 3. (a) NRU test of SA and BetSA in NIH/3T3 cells; (b) IC_{50} values of the NRU test for SA and BetSA in NIH/3T3 cells.

The anti-inflammatory effects of betaine, SA, and BetSA were assessed in a UV-induced keratinocyte inflammation model. UV exposure triggered IL-1α and IL-8 overexpression (NC), which was significantly suppressed in drug-treated groups (PC), validating the model (Fig. 4a-b). BetSA exhibited superior efficacy, markedly reducing IL-1α levels (unlike betaine or SA) and showing stronger IL-8 inhibition compared to SA (Fig. 4a-b). Additionally, BetSA demonstrated robust antioxidant activity, effectively scavenging ROS and enhancing SOD activity (Fig. 4c-d).

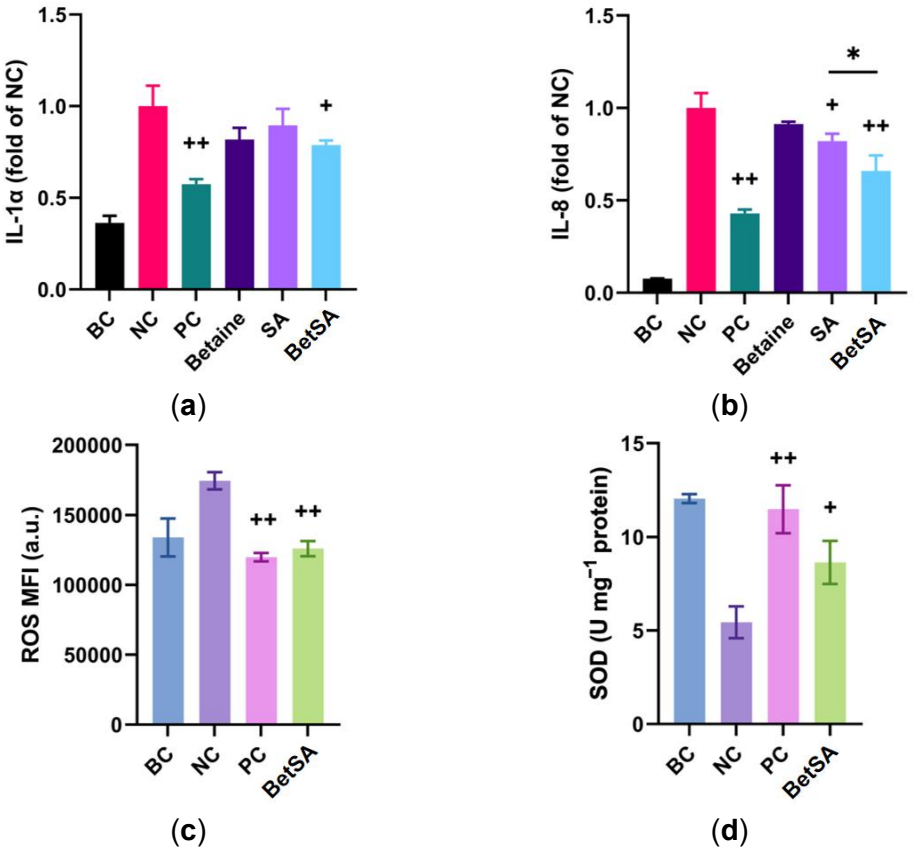

Figure 4. (a-b) Anti-inflammatory effects of betaine, SA, and BetSA; (c-d) Anti-oxidation performance of BetSA. Results are presented as mean ± SD for n=3; ns = no significant difference; *p < 0.05; +p < 0.05, ++p < 0.01 vs. NC.

The efficacy of BetSA in reducing TEWL, porphyrins, erythema, and acne severity significantly exceeded that of Blank by day 28 (Fig. 5-6). Key parameters, including transepidermal water loss (TEWL, skin barrier integrity) [14], porphyrins (sebum/acne biomarkers) [15], and erythema (vascular inflammation) [16], were significantly reduced. By day 28, BetSA achieved reductions of 43.45% (TEWL), 40.80% (porphyrin), 44.37% (erythema), and 37.51% (acne). Blank treatment led to a 21.90%, 26.16%, 24.52%, and 24.01% reduction in TEWL, porphyrin, red lesions, and acne. Furthermore, BetSA also scored higher in self-assessment of oil control, acne reduction, and absorption, leading to a greater likelihood of repurchase, highlighting its considerable market potential.

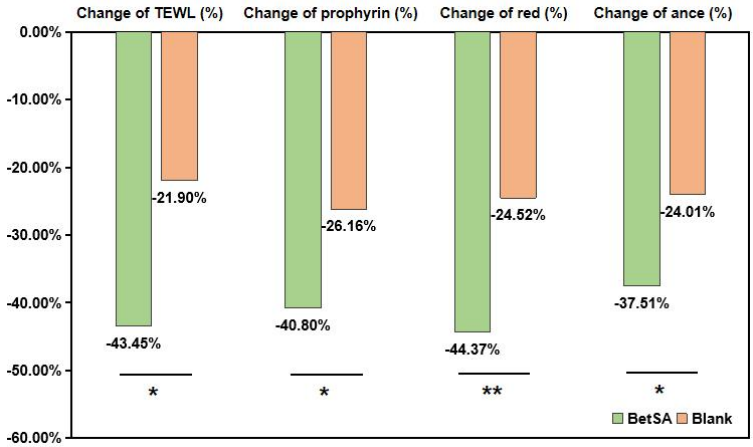

Figure 5. Percentage change in trans epidermal water loss (TEWL), porphyrin, red lesions, and acne levels on subjects' faces after 28 days of treatment with BetSA and Blank. Results are presented as mean ± standard deviation for n=30, *p < 0.05; **p < 0.01.

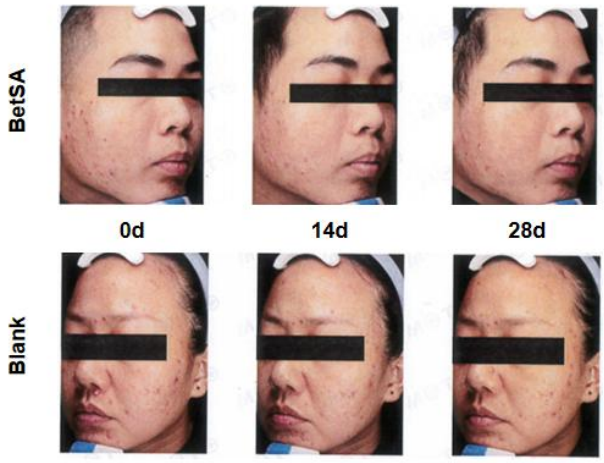

Figure 6. Representative photographs of subjects after treatment with BetSA and Blank.

We also conducted DFT simulations to elucidate the structure-activity relationship of BetSA. The ESP maps revealed that betaine is a polar molecule with a high proportion of polar surface area, consistent with its hydrophilicity, while SA has an ESP distribution more concentrated around zero, consistent with its lipophilicity (Fig. 7).

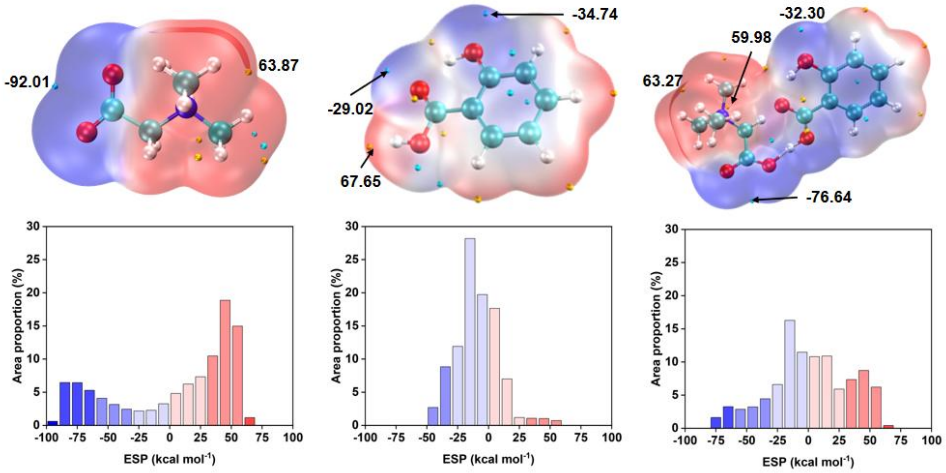

Figure 7. Electrostatic potential (ESP) analysis of betaine, SA, and BetSA.

IGMH analysis indicated that in BetSA, the most positive site of SA forms strong hydrogen bonds with the most negative site of betaine (Fig. 8), thereby reducing the negative potential compared with betaine.

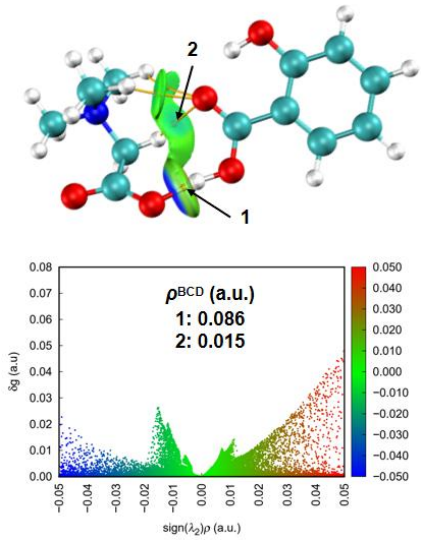

Figure 8. EleIndependent gradient model based on the Hirshfeld partition (IGMH) analysis of BetSA.

The phenolic hydroxyl bond length of BetSA was longer than that of SA, with a greater charge difference at the ends, indicating easier dissociation (Fig. 9a). Both BetSA and SA demonstrated similar antioxidant capabilities in BDE, IP + PDE, and PA + ETE (Figure 9b).

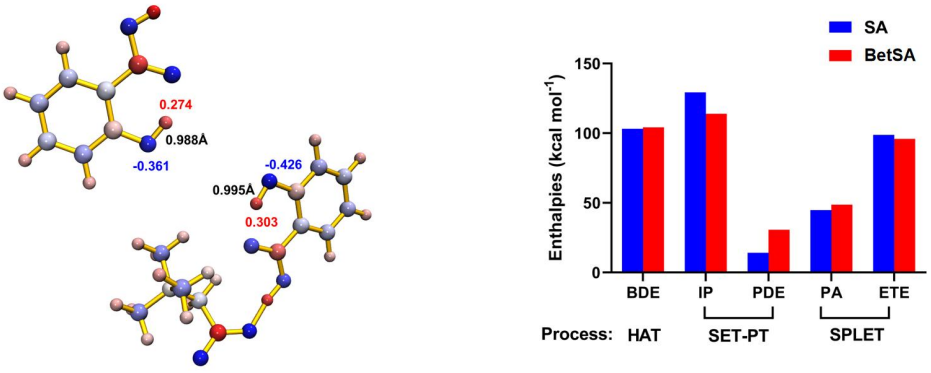

(**a**) (**b**)

Figure 9. (a) Phenolic hydroxyl group analysis of SA and BetSA; (b) Antioxidant ability comparison of SA and BetSA.

Toll-like receptors (TLRs), which are critical mediators of cutaneous immune responses, recognize pathogen-associated molecular patterns (PAMPs) and subsequently activate MyD88/NF-κB signaling pathways to promote the release of inflammatory cytokines [17]. SA alleviates skin inflammation partly by inhibiting NF-κB activity, thereby highlighting TLRs as potential therapeutic targets [18]. Among TLRs, TLR2 and TLR4 play central roles in inflammatory skin diseases and share a conserved Toll/interleukin-1 receptor (TIR) domain that is essential for downstream signaling events [19]. Molecular docking studies and molecular dynamics (MD) simulations reveal that BetSA forms stronger hydrogen bonds with the TIR domain compared to SA (Figures 10a-b). Specifically, BetSA establishes both N−H···O and O−H···O hydrogen bonds with the TIR domain, whereas SA only engages in N−H···O interactions. MD simulations further confirm that BetSA exhibits shorter and stronger hydrogen bonds (Fig. 10c), with the O−H···O bonds demonstrating significantly higher binding energy.

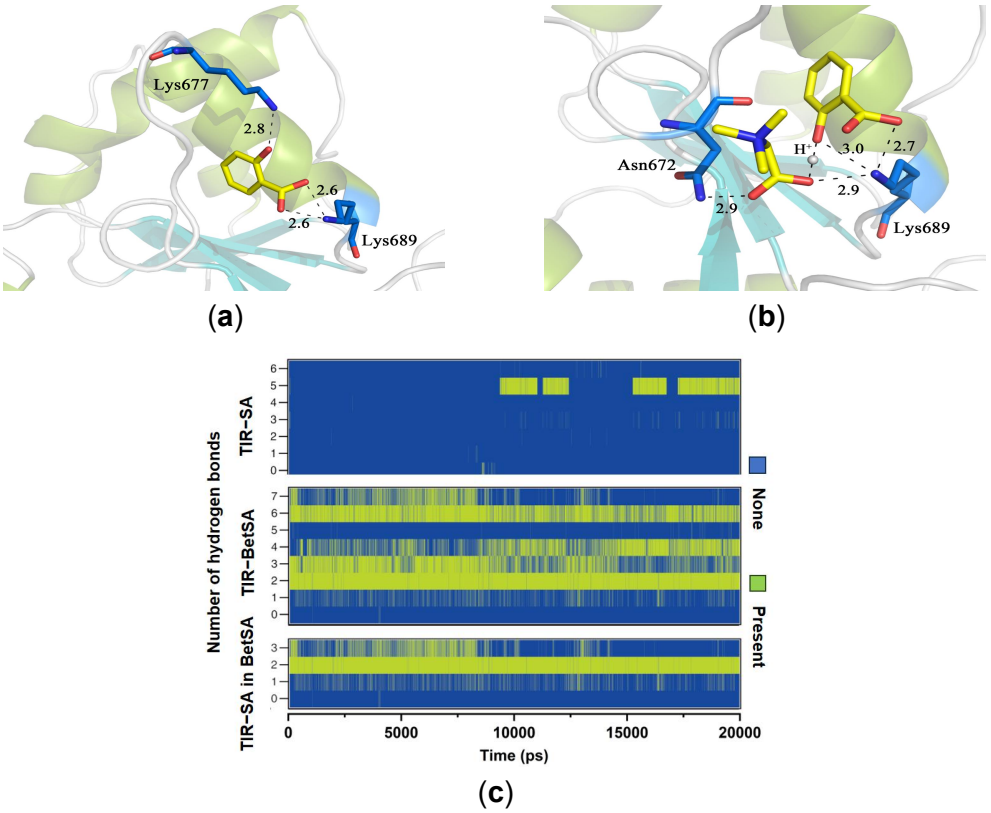

Figure 10. Molecular docking analysis of SA-Toll/interleukin-1 receptor (SA-TIR) and BetSA-Toll/interleukin-1 receptor (BetSA-TIR) complexes. (a-b) Optimized docking results; (c) Structure superposition diagram after molecular dynamics (MD) simulations.

4. Discussion

There exists an intrinsic connection between the physicochemical properties of BetSA and its structure. For instance, in the ^{1}H NMR spectrum (Fig. 1b), compared with betaine, the significant shift in H between the amino and carboxyl groups in BetSA suggests strong hydrogen bonding, which led to a decrease in magnetic shielding around the carboxyl group of betaine. IGMH analysis revealed that in BetSA, the most positively charged region of SA establishes strong hydrogen bonds with the most negatively charged region of betaine (Fig. 8), which is consistent with the observed ^{1}H NMR chemical shift changes (Fig. 1b).

The length of O3-H4 · · · O4 is 1.53 Å in BetSA crystal (Fig. 2a), which is shorter than the intermolecular hydrogen bonds within the SA crystal (1.627 Å). This indicates a stronger hydrogen bonding interaction between betaine and SA, thereby enhancing thermal stability. The interaction between SA and betaine reduces the intramolecular hydrogen bonding of SA and weakens the electrostatic interactions of betaine. Consequently, BetSA exhibits distinct thermal properties compared to SA and betaine (Fig. 1d). BetSA remains liquid over a broader temperature range, facilitating easier processing.In the FTIR spectrum of BetSA, the O-H stretching peak shows a blue shift, while the C=O stretching peak shows a red shift, indicating that the supramolecular interaction between SA and betaine weakens the intramolecular hydrogen bond of SA and the electrostatic interaction of betaine. In BetSA cocrystals, SA still forms an intramolecular hydrogen bond with a length of 1.83 Å, longer than that in SA crystal (1.785 Å), indicating weaker intramolecular hydrogen bonding, consistent with the FTIR results (Fig. 1c).

The bioactivities of BetSA demonstrated low irritation and high anti-inflammatory and antioxidant activities. The reduced irritancy and enhanced anti-inflammatory efficacy of BetSA were attributed to stronger hydrogen bonding with the TIR domain, as revealed by molecular docking and MD simulations (Fig. 10a-b). In addition, the phenolic hydroxyl group of SA plays a significant role in radical scavenging activity [20]. Current radical scavenging mechanisms primarily include: 1) hydrogen atom transfer (HAT), governed by the thermochemical parameter BDE; 2) sequential proton loss electron transfer (SPLET), involving adiabatic ionization potential (IP) and proton dissociation enthalpy (PDE); 3) single-electron transfer-proton transfer (SET-PT), characterized by proton affinity (PA) and electron transfer enthalpy (ETE). DFT calculations revealed that BetSA and SA exhibited comparable antioxidant capabilities in terms of bond dissociation enthalpy (BDE), adiabatic ionization potential combined with proton dissociation enthalpy (IP + PDE), and proton affinity combined with electron transfer enthalpy (PA + ETE) (Figure 9b).This conclusion aligns with the findings that BetSA effectively scavenged reactive oxygen species (ROS) and enhanced superoxide dismutase (SOD) activity (Figure 4c-d).These data also provide compelling evidence that BetSA exhibits significant restorative, antibacterial, anti-inflammatory, and anti-acne effects in clinical trials.

5. Conclusion

This study reports the successful development of a betaine-salicylic acid cocrystal (BetSA) as an innovative solution to address the limitations of conventional SA in acne therapy. Through rational crystal engineering, the distinctive supramolecular architecture of BetSA featuring hydrogen-bonded networks between betaine and SA enhanced its thermal stability, solubility, and biocompatibility while alleviating the irritancy associated with SA. Biological assessments revealed that BetSA exhibited a superior safety profile with significantly reduced cytotoxicity and phototoxicity compared to SA. Clinically, BetSA demonstrated enhanced performance over SA in mitigating acne-related symptoms, improving skin barrier function, and reducing sebum-associated biomarkers, with sustained efficacy over time. This work highlights the potential of cocrystallization as a strategy to optimize bioactive compounds for dermatological applications, achieving a balance between efficacy and safety. Future investigations should focus on the long-term effects of BetSA, its transdermal delivery mechanisms, and scalability, thereby advancing next-generation skincare innovations grounded in supramolecular science.

References

1 J. Lu, T. Cong, X. Wen, X. Li, D. Du, G. He and X. Jiang, Salicylic acid treats acne vulgaris by suppressing AMPK/SREBP 1 pathway in sebocytes, *Experimental dermatology*, 2019, **28**, 786-794.
2 T. Arif, Salicylic acid as a peeling agent: a comprehensive review, *Clinical, cosmetic and investigational dermatology*, 2015, 455-461.
3 A. Durairaj, K. Elumalai and A. Shanmugam, Cystic acne treatment: A comprehensive review, *Medicine Advances*, 2023, **1**, 318-329.
4 X. Zhang, L. Cao, H. Li, Z. Xiong, Z. Fu, Z. Zhang, W. Xie, H. Cui, S. Zhang and Y. Tang, Construction of tea tree oil/salicylic acid/palygorskite hybrids for advanced antibacterial and anti-inflammatory performance, *Journal of Materials Chemistry B*, 2023, **11**, 4260-4273.
5 G. Bolla, B. Sarma and A. K. Nangia, Crystal engineering of pharmaceutical cocrystals in the discovery and development of improved drugs, *Chem Rev*, 2022, **122**, 11514-11603.

6 M. Guo, X. Sun, J. Chen and T. Cai, Pharmaceutical cocrystals: A review of preparations, physicochemical properties and applications, *Acta Pharmaceutica Sinica B*, 2021, **11**, 2537-2564.
7 M. Wang, Z. Wang, J. Zhang, L. Zhang, W. Wang, J. Zhan, Y. Liao, C. Wu, W. Yu and J. Zhang, A matrine-based supramolecular ionic salt that enhances the water solubility, transdermal delivery, and bioactivity of salicylic acid, *Chemical Engineering Journal*, 2023, **468**, 143480.
8 11C. R. Day and S. A. Kempson, Betaine chemistry, roles, and potential use in liver disease, Biochimica et Biophysica Acta (BBA)-General Subjects, 2016, 1860, 1098-1106.
9 V. Filatov, A. Sokolova, N. Savitskaya, M. Olkhovskaya, A. Varava, E. Ilin and E. Patronova, Synergetic Effects of Aloe Vera Extract with Trimethylglycine for Targeted Aquaporin 3 Regulation and Long-Term Skin Hydration, *Molecules*, 2024, **29**, 1540.
10 K. Kim, A. Im, H. Kwon and S. Chae, Betaine promotes LKB1-AMPK activation inhibits UVB-mediated senescence of human epidermal keratinocytes through autophagy induction, *J Mol Genet Med*, 2018, **12**, 1-8.
11 1N. Skroza, E. Tolino, A. Mambrin, S. Zuber, V. Balduzzi, A. Marchesiello, N. Bernardini, I. Proietti and C. Potenza, Adult acne versus adolescent acne: a retrospective study of 1,167 patients, The Journal of clinical and aesthetic dermatology, 2018, 11, 21.
12 T. Lu and Q. Chen, Independent gradient model based on Hirshfeld partition: A new method for visual study of interactions in chemical systems, *Journal of Computational Chemistry*, 2022, **43**, 539-555.
13 Y. Li, L. Chen, Y. Sun, R. Wang, B. Zhao and T. Jing, Exploring the effect of surfactants on the interaction between laccase and bisphenol A by molecular docking, molecular dynamics, and energy calculations, *Journal of Molecular Liquids*, 2023, **382**, 121928.
14 Q. Jiao, L. Yue, L. Zhi, Y. Qi, J. Yang, C. Zhou and Y. Jia, Studies on stratum corneum metabolism: function, molecular mechanism and influencing factors, *Journal of Cosmetic Dermatology*, 2022, **21**, 3256-3264.
15 L. Verde, E. Frias-Toral, S. Cacciapuoti, D. Simancas-Racines, M. Megna, G. Caiazzo, L. Potestio, M. Maisto, G. C. Tenore and A. Colao, Very low-calorie ketogenic diet (VLCKD): a therapeutic nutritional tool for acne?, *Journal of Translational Medicine*, 2024, **22**, 322.
16 Y. Ji, H. Li, J. Li, G. Yang, W. Zhang, Y. Shen, B. Xu, J. Liu, J. Wen and W. Song, Hair Follicle-Targeted Delivery of Azelaic Acid Micro/Nanocrystals Promote the Treatment of Acne Vulgaris, *International Journal of Nanomedicine*, 2024, 5173-5191.
17 V. Kumar, Going, Toll-like receptors in skin inflammation and inflammatory diseases, EXCLI journal, 2021, 20, 52.
18 L. Sun, W. Liu and L.-j. Zhang, The role of toll‐like receptors in skin host defense, psoriasis, and atopic dermatitis, Journal of immunology research, 2019, 2019, 1824624.
19 S. Chen, R. Lin, H. Lu, Q. Wang, J. Yang, J. Liu and C. Yan, Effects of phenolic acids on free radical scavenging and heavy metal bioavailability in kandelia obovata under cadmium and zinc stress, Chemosphere, 2020, 249, 126341.
20 Z. Marković, J. Tošović, D. Milenković and S. Marković, Revisiting the solvation enthalpies and free energies of the proton and electron in various solvents, Computational and Theoretical Chemistry, 2016, 1077, 11-17.